

A pointwise limit theorem for filtered backprojection in computed tomography

Yangbo Ye^{a)}

Department of Mathematics, University of Iowa, Iowa City, Iowa 52242

Jiehua Zhu^{b)}

Department of Mathematics, University of Iowa, Iowa City, Iowa 52242

Ge Wang^{c)}

Departments of Mathematics, Biomedical Engineering, and Radiology, University of Iowa, Iowa City, Iowa 52242

(Received 16 September 2002; accepted for publication 14 January 2003; published 22 April 2003)

Computed tomography (CT) is one of the most important areas in the modern science and technology. The most popular approach for image reconstruction is filtered backprojection. It is essential to understand the limit behavior of the filtered backprojection algorithms. The classic results on the limit of image reconstruction are typically done in the norm sense. In this paper, we use the method of limited bandwidth to handle filtered backprojection-based image reconstruction when the spectrum of an underlying image is not absolutely integrable. Our main contribution is, assuming the method of limited bandwidth, to prove a pointwise limit theorem for a class of functions practically relevant and quite general. Further work is underway to extend the theory and explore its practical applications. © 2003 American Association of Physicists in Medicine. [DOI: 10.1118/1.1559820]

Key words: computed tomography (CT), image reconstruction, filtered backprojection, error analysis, limited bandwidth, pointwise limit

I. INTRODUCTION

Computed tomography (CT) is one of the most important areas in modern science and technology. The most popular approach for image reconstruction is filtered backprojection.^{1,2} Let $f(x,y)$ be an absolutely integrable function on R^2 representing an object with a finite support, such as defined on a unit disk. In this context, the standard procedure for computed tomography (CT) refers to the following steps:

Step 1. Projection:

$$P_{\theta}(t) = \int_{-\infty}^{\infty} \int_{-\infty}^{\infty} f(x,y) \delta(x \cos \theta + y \sin \theta - t) dx dy, \quad (1)$$

Step 2. Filtration:

$$Q_{\theta}(t) = \int_{-\infty}^{\infty} S_{\theta}(w) |w| e^{2\pi i w t} dw, \\ \text{where } S_{\theta}(w) = \int_{-\infty}^{\infty} P_{\theta}(t) e^{-2\pi i w t} dt, \quad (2)$$

Step 3. Backprojection:

$$f(x,y) = \int_0^{\pi} Q_{\theta}(x \cos \theta + y \sin \theta) d\theta. \quad (3)$$

The correctness of the above procedure is usually shown by citing the Fourier slice theorem that

$$S_{\theta}(w) = \hat{f}(w \cos \theta, w \sin \theta) \\ = \int_{-\infty}^{\infty} \int_{-\infty}^{\infty} f(x,y) e^{-2\pi i(xw \cos \theta + yw \sin \theta)} dx dy. \quad (4)$$

Rigorously speaking, the filtered backprojection algorithm defined by (2) and (3) is valid at almost every point (x,y) for an absolutely integrable function $f(x,y)$, when its Fourier transform $\hat{f}(u,v)$ is also absolutely integrable.

When $\hat{f}(u,v)$ is not absolutely integrable, it is essential to understand the limit behavior of the filtered backprojection algorithms. There are various strategies to handle this divergence problem. Examples include the method of limited bandwidth,¹ the Abel method of summability,¹ and the Shepp–Logan filter technique.⁸ Generally speaking, different strategies have their own advantages and disadvantages. As a matter of fact, CT scanner manufacturers typically implement a number of reconstruction filters to balance spatial and contrast resolution for different applications. Typically, the method of limited bandwidth produces higher spatial resolution, while the Abel method of summability and the Shepp–Logan filtering lead to better contrast resolution. The convolution kernel associated with the method of limited bandwidth is usually referred to as the “standard” kernel, while the smooth kernels associated with the Shepp–Logan method and other similar methods may be regarded as “contrast” kernels.

The Abel method of summability is to introduce a convergence factor $e^{-\epsilon|w|}$, and then take $\epsilon \rightarrow 0^+$:

$$Q_{\theta,\epsilon}(t) = \int_{-\infty}^{\infty} S_{\theta}(w)|w|e^{-\epsilon|w|}e^{2\pi itw} dw, \tag{5}$$

$$f_{\epsilon}(x,y) = \int_0^{\pi} Q_{\theta,\epsilon}(x \cos \theta + y \sin \theta) d\theta \tag{6}$$

for $\epsilon > 0$, and

$$f(x,y) = \lim_{\epsilon \rightarrow 0} f_{\epsilon}(x,y). \tag{7}$$

For any absolutely integrable function $f(x,y)$, it is a classical result that $f_{\epsilon}(x,y)$ tends to $f(x,y)$ in the L^1 norm as $\epsilon \rightarrow 0$:

$$\lim_{\epsilon \rightarrow 0} \int_{-\infty}^{\infty} \int_{-\infty}^{\infty} |f_{\epsilon}(x,y) - f(x,y)| dx dy = 0. \tag{8}$$

Using the concept of the Lebesgue set of $f(x,y)$, we can further prove that $f_{\epsilon}(x,y)$ tends to $f(x,y)$ as $\epsilon \rightarrow 0$ almost everywhere.³

It is our goal in the present paper to study the limit behavior of the method of limited bandwidth. This method is to assume that the bandwidth is limited and replace (2) and (3) by (9) and (10):

$$Q_{\theta,W}(t) = \int_{-W}^W S_{\theta}(w)|w|e^{2\pi itw} dw, \tag{9}$$

$$f_W(x,y) = \int_0^{\pi} Q_{\theta,W}(x \cos \theta + y \sin \theta) d\theta. \tag{10}$$

Then, we take the limit to reconstruct the image $f(x,y)$:

$$f(x,y) = \lim_{W \rightarrow \infty} f_W(x,y). \tag{11}$$

As far as the method of limited bandwidth defined in (9)–(11) is concerned, a corresponding L^1 statement does not exist.

In fact, (9) can be written as

$$Q_{\theta,W}(t) = \int_{-\infty}^{\infty} S_{\theta}(w)\Phi(w/W)|w|e^{2\pi itw} dw, \tag{12}$$

where Φ is the characteristic function of the interval $[-1,1]$, which can be interpreted as the characteristic function in polar coordinates on the unit disk $x^2 + y^2 \leq 1$. Consequently, $f_W(x,y)$ is the Fourier inversion of $\hat{f}(u,v)\Phi(u/W,v/W)$. By the Fourier convolution formula,

$$f_W(x,y) = f(x,y) * (\Phi(u/W,v/W))^{\wedge}, \tag{13}$$

where $(\Phi(u/W,v/W))^{\wedge}$ is expressed as follows:

$$\begin{aligned} (\Phi(u/W,v/W))^{\wedge}(x,y) &= \int_{-\infty}^{\infty} \int_{-\infty}^{\infty} \Phi(u/W,v/W) \\ &\quad \times e^{-2\pi i(xu+yv)} du dv \\ &= W^2 \hat{\Phi}(xW,yW). \end{aligned} \tag{14}$$

Here in polar coordinates,

$$\hat{\Phi}(w \cos \theta, w \sin \theta) = J_1(2\pi w)/w$$

is not absolutely integrable on the plane, where J_1 is the Bessel function of the first kind of order one [see (20) below]. Therefore, $f_W(x,y)$ in (13) is not of L^1 in general. We need an L^2 theory to describe the limit behavior of the limited bandwidth based reconstruction in (11).

Assume $f \in L^1(R^2) \cap L^2(R^2)$, then $\hat{f} \in L^2(R^2)$. The Fourier transform of an L^2 function g is defined as the L^2 limit of

$$\begin{aligned} \hat{g}_W(x,y) &= \int_{-\infty}^{\infty} \int_{-\infty}^{\infty} g(u,v)\Phi(u/W,v/W) \\ &\quad \times e^{-2\pi i(ux+vy)} du dv. \end{aligned} \tag{15}$$

By the Plancherel theorem,³ we immediately have

$$\lim_{W \rightarrow \infty} \int_{-\infty}^{\infty} \int_{-\infty}^{\infty} |f_W(x,y) - f(x,y)|^2 dx dy = 0. \tag{16}$$

Similar to (16), the classic results on the limit of image reconstruction are typically done in the norm sense. The most famous results are summarized in the book by Natterer.² Specifically, they worked with C^∞ and assumed the sup norm defined on $H_0^\beta(\Omega^n)$ as the worst-case error. The only prior information they made use of is $\|f\|_{H_0^\beta(\Omega^n)} \leq \rho$, with β being about 1/2 and ρ moderate (see pp. 92–95 in Ref. 2 for details).

In this paper, we study the method of limited bandwidth to handle filtered backprojection based image reconstruction when the spectrum of an underlying image is not absolutely integrable. Particularly, assuming the method of a limited bandwidth we prove a pointwise limit theorem for a class of functions practically relevant and quite general. In the second section, we present our main result—the pointwise limit theorem. In the third section, we give two analytic examples, while in the last section, we discuss several issues and conclude the paper.

II. POINTWISE LIMIT THEOREM

Because the pointwise limit is stronger and much more specific than the L^2 limit, in this section we prove a pointwise limit theorem to refine (16) for a class of quite general functions $f(x,y)$. Indeed, we will consider functions $f(x,y)$ that are smooth but have finitely many jumps of finite magnitude along piecewise continuous curves.

Theorem 1 (pointwise limit theorem): *Let $f(x,y)$ be an absolutely integrable function on R^2 . Assume that, other than finitely many jumps of finite magnitude of the function and/or its first and second partial derivatives along piecewise continuous curves, this function has absolutely integrable second partial derivatives. Then, the filtered backprojection using the method of limited bandwidth converges pointwise at any point (x_0,y_0) not on a jump, i.e.,*

$$\lim_{W \rightarrow \infty} f_W(x_0,y_0) = f(x_0,y_0).$$

We remark that in the scenario of medical imaging, there are distinctive components in the human body, including solid organs, soft tissues, bones, and so on. Within each compo-

ment, the x-ray linear attenuation coefficient varies smoothly, and can be well modeled by smooth functions with continuous second derivatives. On the other hand, across the boundaries among the components, jumps in the x-ray linear attenuation coefficient, its first and second partial derivatives can be represented by a finite number of gate-like functions. The discontinuities across the boundaries in the first and second derivatives can be relevant in contrast dynamics, such as bolus-driven perfusion for cancer studies.

Before we prove Theorem 1, let us formulate this class of functions. As we will use polar coordinates centered at (x_0, y_0) in our proof, we express the curves of discontinuities in the following way. Note that this expression of our function $f(x, y)$ directly depends on a given point (x_0, y_0) not on a jump. For a different point (x_0, y_0) , the polar coordinates will be different, and the formulas for the function $f(x_0 - r \cos \theta, y_0 - r \sin \theta)$ will also be different.

Without a loss of generality, let $r = r_j(\theta)$, $j = 1, \dots, m$, be piecewise continuous curves in θ . We may further assume that $0 < r_1(\theta) < r_2(\theta) < \dots < r_m(\theta) \leq C_1$ for any θ . To capture various jumps of the function and its derivatives on these curves, we use a polynomial of r in the region between two adjacent curves. More precisely, define jump functions:

$$h_j(r, \theta) = \begin{cases} a_j^{(0)}(\theta) + a_j^{(1)}(\theta)r + \dots + a_j^{(5)}(\theta)r^5, & \text{if } r_j(\theta) \leq r < r_{j+1}(\theta), \\ 0, & \text{otherwise,} \end{cases} \quad (17)$$

for $j = 1, \dots, m-1$, where as coefficients, $a_j^{(k)}(\theta)$ are bounded, $|a_j^{(k)}(\theta)| \leq C_2$, piecewise continuous functions of θ . Here we use a polynomial of degree 5, because we need to use six coefficients $a_j^{(k)}(\theta)$ to match the function values, its first and second derivatives in the direction of r on the outer and inner rims of the region between $r_j(\theta)$ and $r_{j+1}(\theta)$. We remark that our jump function in (17) generalizes the gate function,

$$s_j(r, \theta) = \begin{cases} a_j^{(0)}(\theta), & \text{if } r_j(\theta) \leq r < r_{j+1}(\theta), \\ 0, & \text{otherwise.} \end{cases}$$

This generalization allows us to control jumps, not only in value magnitude but also in derivatives. For our function $f(x, y)$ in Theorem 1, we request that in polar coordinates centered at the point (x_0, y_0) , it can be written as

$$\begin{aligned} f(x_0 - r \cos \theta, y_0 - r \sin \theta) &= g(x_0 - r \cos \theta, y_0 - r \sin \theta) + h_1(r, \theta) + \dots \\ &+ h_{m-1}(r, \theta) \end{aligned} \quad (18)$$

such that (i) $g(x, y)$ is absolutely integrable on R^2 , (ii) $g(x, y)$ has all second partial derivatives everywhere in R^2 , and (iii) its second partial derivatives are also absolutely integrable on R^2 . Note that on the right side of (18), the second differentiability of $g(x, y)$ on jump curves is achieved by suitably choosing the coefficients $a_j^{(k)}(\theta)$ of the polynomials $h_j(r, \theta)$.

Actually, we may replace conditions (ii) and (iii) by a weaker condition that

$$\int_0^{2\pi} [g(x_0 - r \cos \theta, y_0 - r \sin \theta)]_{\cos}^{\wedge}(t) d\theta = O(t^{-1-\epsilon}), \quad (19)$$

for some fixed $\epsilon > 0$ as $t \rightarrow \infty$. Here we used the Fourier cosine transform,

$$\hat{g}_{\cos}(t) \equiv \int_0^{\infty} g(r) \cos(rt) dr.$$

The assumption (19) essentially means that the Fourier cosine transform of $g(x, y)$, along any half-line starting at (x_0, y_0) , goes to 0 in $O(t^{-1-\epsilon})$, as $t \rightarrow \infty$. This is a version of the Riemann–Lebesgue theorem.⁴ If, as in Theorem 1, $g(x, y)$ has absolutely integrable second partial derivatives, the bound in (19) will be $O(t^{-2})$.

The magnitude of the jumps cannot be allowed to go to infinity, as controlled by $|a_j^{(k)}(\theta)| \leq C_2$ for $j = 1, \dots, m-1$ and $k = 0, \dots, 5$. The jumps cannot occur at the point (x_0, y_0) either, so that $r_j(\theta)$ cannot approach to 0. If we denote by $c = c(x_0, y_0) > 0$ the shortest distance from (x_0, y_0) to the nearest discontinuous curve, we then have $|r_j(\theta)| \geq c(x_0, y_0)$.

We emphasize that the class of the above-defined functions $f(x, y)$ in (18) should be regarded as a universal model for a variety of practical applications. Technically, $g(x_0 - r \cos \theta, y_0 - r \sin \theta)$ is smooth and describes continuous changes in the image domain, while terms $h_j(r, \theta)$ capture the structural discontinuities. Combining the two kinds of bases, we can satisfactorily approximate images that are regionwise smooth.

In the proof below and in later sections, we will use the Bessel function J_n of order n of the first kind and the Gauss hypergeometric series ${}_2F_1$, defined as

$$J_n(z) = \frac{1}{2\pi} \int_0^{2\pi} e^{i(z \sin t - nt)} dt \quad (20)$$

and

$$\begin{aligned} &{}_2F_1(a, b; c; z) \\ &= 1 + \sum_{n=1}^{\infty} \frac{a(a+1) \cdots (a+n-1) b(b+1) \cdots (b+n-1)}{c(c+1) \cdots (c+n-1) n!} z^n. \end{aligned}$$

See Ref. 6 for details.

Proof of Theorem 1: By (13), we have

$$\begin{aligned} f_W(x_0, y_0) &= f(x, y) * (W^2 \hat{\Phi}(xW, yW))|_{(x_0, y_0)} \\ &= W^2 \int_{-\infty}^{\infty} \int_{-\infty}^{\infty} f(x_0 - x, y_0 - y) \\ &\quad \times \hat{\Phi}(xW, yW) dx dy. \end{aligned} \quad (21)$$

In polar coordinates, it is

$$\begin{aligned}
 f_W(x_0, y_0) &= W^2 \int_0^{2\pi} d\theta \int_0^\infty f(x_0 - r \cos \theta, y_0 - r \sin \theta) \\
 &\quad \times J_1(2\pi r W) \frac{r dr}{r W} \\
 &= W \int_0^{2\pi} d\theta \int_0^\infty f(x_0 - r \cos \theta, y_0 - r \sin \theta) \\
 &\quad \times J_1(2\pi r W) dr \\
 &= \frac{1}{2\pi} \int_0^{2\pi} d\theta \\
 &\quad \times \int_0^\infty f\left(x_0 - \frac{t \cos \theta}{2\pi W}, y_0 - \frac{t \sin \theta}{2\pi W}\right) J_1(t) dt.
 \end{aligned}
 \tag{22}$$

Recall the Parseval formula for absolute integrable functions f and g on $[0, \infty)$:

$$\int_0^\infty f(t) \hat{g}_{\cos}(t) dt = \int_0^\infty \hat{f}_{\cos}(t) g(t) dt.
 \tag{23}$$

It is known that⁵

$$\hat{(J_1)}_{\cos}(t) = \begin{cases} 1, & 0 < t < 1; \\ 1 - \frac{t}{\sqrt{t^2 - 1}}, & t > 1. \end{cases}
 \tag{24}$$

Denote the function on the right side as $g(t)$. Then, by the inversion formula of the Fourier cosine transform,

$$J_1(t) = \left(\frac{2}{\pi} g\right)_{\cos}^\wedge(t).
 \tag{25}$$

Consequently,

$$\begin{aligned}
 f_W(x_0, y_0) &= \frac{1}{2\pi} \int_0^{2\pi} d\theta \int_0^\infty f\left(x_0 - \frac{r \cos \theta}{2\pi W}, y_0 - \frac{r \sin \theta}{2\pi W}\right)_{\cos}^\wedge(t) \frac{2}{\pi} g(t) dt \\
 &= \frac{1}{\pi^2} \int_0^{2\pi} d\theta \int_0^\infty f\left(x_0 - \frac{r \cos \theta}{2\pi W}, y_0 - \frac{r \sin \theta}{2\pi W}\right)_{\cos}^\wedge(t) dt - \frac{1}{\pi^2} \int_0^{2\pi} d\theta \int_1^\infty f\left(x_0 - \frac{r \cos \theta}{2\pi W}, y_0 - \frac{r \sin \theta}{2\pi W}\right)_{\cos}^\wedge(t) \frac{t dt}{\sqrt{t^2 - 1}} \\
 &= f(x_0, y_0) - \frac{2W}{\pi} \int_0^{2\pi} d\theta \int_1^\infty (f(x_0 - r \cos \theta, y_0 - r \sin \theta))_{\cos}^\wedge(2\pi W t) \frac{t dt}{\sqrt{t^2 - 1}}.
 \end{aligned}
 \tag{26}$$

If for a fixed $\epsilon > 0$, $\int_0^{2\pi} (g(x_0 - r \cos \theta, y_0 - r \sin \theta))_{\cos}^\wedge(t) d\theta = O(1/t^{1+\epsilon})$, then we have

$$\begin{aligned}
 & - \frac{2W}{\pi} \int_0^{2\pi} d\theta \int_1^\infty (g(x_0 - r \cos \theta, y_0 - r \sin \theta))_{\cos}^\wedge(2\pi W t) \\
 & \quad \times \frac{t dt}{\sqrt{t^2 - 1}} \leq \frac{1}{W^\epsilon} \int_1^\infty \frac{dt}{t^\epsilon \sqrt{t^2 - 1}},
 \end{aligned}
 \tag{27}$$

which converges and tends to 0 as $W \rightarrow \infty$. Consequently, the contribution to (26) of the term g in the expression of $f(x_0 - r \cos \theta, y_0 - r \sin \theta)$ in (18) will tend to 0. As for the terms $a_j^{(k)}(\theta) r^k$ in $h_j(r, \theta)$ on the right side of (18), we have the following computation:

$$(a_j^{(0)}(\theta) u_j(r))_{\cos}^\wedge(x) = a_j^{(0)}(\theta) \frac{\sin(r_{j+1}(\theta)x) - \sin(r_j(\theta)x)}{x},$$

$$\begin{aligned}
 & (a_j^{(1)}(\theta) r u_j(r))_{\cos}^\wedge(x) \\
 & = a_j^{(1)}(\theta) \frac{d}{dx} \frac{\cos(r_j(\theta)x) - \cos(r_{j+1}(\theta)x)}{x},
 \end{aligned}$$

$$\begin{aligned}
 & (a_j^{(2)}(\theta) r^2 u_j(r))_{\cos}^\wedge(x) \\
 & = a_j^{(2)}(\theta) \frac{d^2}{dx^2} \frac{\sin(r_j(\theta)x) - \sin(r_{j+1}(\theta)x)}{x},
 \end{aligned}$$

$$\begin{aligned}
 & (a_j^{(3)}(\theta) r^3 u_j(r))_{\cos}^\wedge(x) \\
 & = a_j^{(3)}(\theta) \frac{d^3}{dx^3} \frac{\cos(r_{j+1}(\theta)x) - \cos(r_j(\theta)x)}{x},
 \end{aligned}$$

$$\begin{aligned}
 & (a_j^{(4)}(\theta) r^4 u_j(r))_{\cos}^\wedge(x) \\
 & = a_j^{(4)}(\theta) \frac{d^4}{dx^4} \frac{\sin(r_{j+1}(\theta)x) - \sin(r_j(\theta)x)}{x},
 \end{aligned}$$

$$\begin{aligned}
 & (a_j^{(5)}(\theta) r^5 u_j(r))_{\cos}^\wedge(x) \\
 & = a_j^{(5)}(\theta) \frac{d^5}{dx^5} \frac{\cos(r_j(\theta)x) - \cos(r_{j+1}(\theta)x)}{x},
 \end{aligned}$$

where $u_j(r) = 1$ for $r_j(\theta) \leq r < r_{j+1}(\theta)$ and vanishes elsewhere. Consequently,

$$(a_j^{(k)}(\theta)r^k u_j(r))_{\cos(x)}^{\wedge} = \frac{a_j^{(k)}(\theta)}{x} ((r_{j+1}(\theta))^k \sin(r_{j+1}(\theta)x) - (r_j(\theta))^k \sin(r_j(\theta)x)) + \dots, \quad (28)$$

for $k=0, \dots, 5$, where “...” represents terms with x^2 or higher powers of x in the denominators. These omitted terms will contribute expressions tending to 0 when $W \rightarrow \infty$, as in (27). The leading term in (28) in turn contributes,

$$\begin{aligned} & \frac{1}{\pi^2} \int_0^{2\pi} a_j^{(k)}(\theta) (r_j(\theta))^k d\theta \int_1^\infty \frac{\sin(2\pi r_j(\theta)Wt)}{\sqrt{t^2-1}} dt \\ & - \frac{1}{\pi^2} \int_0^{2\pi} a_{j+1}^{(k)}(\theta) (r_{j+1}(\theta))^k d\theta \\ & \times \int_1^\infty \frac{\sin(2\pi r_{j+1}(\theta)Wt)}{\sqrt{t^2-1}} dt \\ & = \frac{1}{2\pi} \int_0^{2\pi} a_j^{(k)}(\theta) (r_j(\theta))^k J_0(2\pi r_j(\theta)W) d\theta \\ & - \frac{1}{2\pi} \int_0^{2\pi} a_{j+1}^{(k)}(\theta) (r_{j+1}(\theta))^k J_0(2\pi r_{j+1}(\theta)W) d\theta. \end{aligned} \quad (29)$$

Recall that we assumed that $a_j(\theta)$ and $r_j(\theta)$ are piecewise continuous and bounded: $|a_j(\theta)| \leq C_2$, $0 < c(x_0, y_0) \leq r_j(\theta) \leq C_1$, for $0 \leq \theta \leq 2\pi$. Consequently, using the asymptotic expansion

$$J_0(z) = \sqrt{\frac{2}{\pi z}} \cos(z - \pi/4) + O(|z|^{-3/2}), \quad (30)$$

we obtain a bound $O(C_1^k C_2^k / \sqrt{c(x_0, y_0)W})$ for (29), which tends to 0 as $W \rightarrow \infty$. The theorem then follows immediately.

III. EXAMPLES

A. Disk function

Theorem 1 covers the characteristic function on the unit disk,

$$f(x, y) = \begin{cases} 1, & x^2 + y^2 \leq 1, \\ 0, & \text{otherwise.} \end{cases} \quad (31)$$

Its Fourier transform

$$\hat{f}(w \cos \theta, w \sin \theta) = S_\theta(w) = \frac{J_1(2\pi w)}{w} \quad (32)$$

is not absolutely integrable over the plane. Now (9) becomes

$$\begin{aligned} Q_{\theta, w}(t) &= \int_{-W}^W S_\theta(w) |w| e^{2\pi i t w} dw \\ &= \int_{-W}^W \frac{|w|}{w} J_1(2\pi w) e^{2\pi i w t} dw \\ &= 2 \int_0^W J_1(2\pi w) \cos(2\pi t w) dw. \end{aligned} \quad (33)$$

According to (10), we have

$$\begin{aligned} f_W(x, y) &= \int_0^\pi Q_{\theta, w}(x \cos \theta + y \sin \theta) d\theta \\ &= 2 \int_0^\pi d\theta \int_0^W J_1(2\pi w) \\ &\quad \times \cos(2\pi w(x \cos \theta + y \sin \theta)) dw. \end{aligned} \quad (34)$$

When $(x, y) \neq (0, 0)$, we may express $x \cos \theta + y \sin \theta$ as $\sqrt{x^2 + y^2} \sin(\theta + \theta_0)$ for a certain phase shifting θ_0 . Changing variables, we have

$$\begin{aligned} f_W(x, y) &= 2 \int_0^\pi d\theta \int_0^W J_1(2\pi w) \cos(2\pi w \sqrt{x^2 + y^2} \sin \theta) dw \\ &= \frac{1}{\pi} \int_0^\pi d\theta \int_0^{2\pi W} J_1(w) \cos(w \sqrt{x^2 + y^2} \sin \theta) dw. \end{aligned} \quad (35)$$

Switch the order of integration,

$$\begin{aligned} f_W(x, y) &= \frac{1}{\pi} \int_0^{2\pi W} J_1(w) dw \int_0^\pi \cos(w \sqrt{x^2 + y^2} \sin \theta) d\theta \\ &= \int_0^{2\pi W} J_1(w) J_0(w \sqrt{x^2 + y^2}) dw. \end{aligned} \quad (36)$$

When $(x, y) = (0, 0)$, (36) is also true.

If $x^2 + y^2 \neq 1$, we have the discontinuous integral of Weber–Schafheitlin as the limit

$$\begin{aligned} \lim_{W \rightarrow \infty} f_W(x, y) &= \int_0^\infty J_1(w) J_0(w \sqrt{x^2 + y^2}) dw \\ &= \begin{cases} 1, & x^2 + y^2 < 1, \\ 0, & x^2 + y^2 > 1. \end{cases} \end{aligned} \quad (37)$$

Therefore,

$$\lim_{W \rightarrow \infty} f_W(x, y) = f(x, y), \quad (38)$$

for points (x, y) not on the unit circle. If $x^2 + y^2 = 1$, we have

$$\int_0^{2\pi W} J_1(w) J_0(w) dw = \frac{1}{2} (1 - J_0^2(2\pi W)). \quad (39)$$

Hence for $x^2 + y^2 = 1$,

$$\lim_{W \rightarrow \infty} f_W(x, y) = \lim_{W \rightarrow \infty} \frac{1}{2} (1 - J_0^2(2\pi W)) = \frac{1}{2}. \quad (40)$$

B. Delta function

If we apply the band-limited reconstruction algorithm (9) and (10) to the Dirac delta function $f(x, y) = \delta(x, y)$, the resultant $\delta_W(x, y)$ exhibits interesting singular behaviors. In fact,

$$\hat{\delta}(w \cos \theta, w \sin \theta) = S_\theta(w) = 1. \quad (41)$$

If $t \neq 0$, we have

$$\begin{aligned} Q_{\theta,W}(t) &= \int_{-W}^W |w| e^{2\pi i t w} dw \\ &= \frac{W \sin(2\pi Wt)}{\pi t} - \frac{\sin^2(\pi Wt)}{\pi^2 t^2}. \end{aligned} \tag{42}$$

When $(x,y) \neq (0,0)$,

$$\begin{aligned} \delta_W(x,y) &= \int_0^\pi Q_{\theta,W}(x \cos \theta + y \sin \theta) d\theta \\ &= \int_0^\pi \left[\frac{W \sin(2\pi \sqrt{x^2+y^2} W \sin \eta)}{\pi \sqrt{x^2+y^2} \sin \eta} - \frac{\sin^2(\pi \sqrt{x^2+y^2} W \sin \eta)}{\pi^2 (x^2+y^2) \sin^2 \eta} \right] d\eta, \end{aligned} \tag{43}$$

by changing variables. Denote $A = \pi \sqrt{x^2+y^2}$ and $t = \sin \eta$. The integrand then equals

$$\frac{W \sin(2AWt)}{At} - \frac{\sin^2(AWt)}{A^2 t^2} = 2W^2 \sum_{n \geq 0} \frac{(-1)^n (2AWt)^{2n}}{(2n)!(2n+2)}. \tag{44}$$

Integrating it termwise, we obtain

$$\begin{aligned} \delta_W(x,y) &= \frac{\pi W}{A} \sum_{n \geq 0} \frac{(-1)^n (AW)^{2n+1}}{n!(n+1)!} \\ &= \frac{\pi W}{A} J_1(2AW) = \frac{W}{\sqrt{x^2+y^2}} J_1(2\pi W \sqrt{x^2+y^2}), \end{aligned} \tag{45}$$

if $(x,y) \neq (0,0)$. On the other hand, it is easy to find that

$$\delta_W(0,0) = \pi W^2. \tag{46}$$

For a given point $(x,y) \neq (0,0)$, we may use the asymptotic expansion

$$J_1(z) = \sqrt{\frac{2}{\pi z}} \cos\left(z - \frac{3\pi}{4}\right) + O\left(\frac{1}{|z|^{3/2}}\right), \tag{47}$$

and derive an asymptotic expansion of (45) as $W \rightarrow \infty$:

$$\begin{aligned} \delta_W(x,y) &= \frac{\sqrt{W}}{\pi(x^2+y^2)^{3/4}} \cos\left(2\pi W \sqrt{x^2+y^2} - \frac{3\pi}{4}\right) \\ &\quad + O\left(\frac{1}{W^{1/2}(\pi \sqrt{x^2+y^2})^{5/2}}\right). \end{aligned} \tag{48}$$

Consequently, in addition to $\lim_{W \rightarrow \infty} \delta_W(0,0) = \infty$ according to (46), $\delta_W(x,y)$ will have a larger and larger magnitude \sqrt{W} of vibration at any fixed location $(x,y) \neq (0,0)$ as $W \rightarrow \infty$.

Nevertheless, $\delta_W(x,y)$ indeed approaches $\delta(x,y)$ as $W \rightarrow \infty$ in the following sense that for a function $f(x,y)$ as in Theorem 1,

$$\lim_{W \rightarrow \infty} \int_{-\infty}^{\infty} \int_{-\infty}^{\infty} f(x_0+x, y_0+y) \delta_W(x,y) dx dy = f(x_0, y_0), \tag{49}$$

where the point (x_0, y_0) satisfies the requirement in Theorem 1. This is because the integral on the left-hand side of (49) is actually equal to $f_W(x_0, y_0)$, and Theorem 1 applies. In particular,

$$\begin{aligned} \int_{-\infty}^{\infty} \int_{-\infty}^{\infty} \delta_W(x,y) dx dy &= \int_0^{2\pi} d\theta \int_0^W \frac{J_1(2\pi W r)}{r} r dr \\ &= 2\pi W \int_0^W J_1(2\pi W r) dr \\ &= \int_0^\infty J_1(z) dz = 1. \end{aligned} \tag{50}$$

It is interesting to compare $\delta_W(x,y)$ with $\delta_\epsilon(x,y)$ obtained by the Abel method of summability:

$$\delta_\epsilon(x,y) = \frac{2\pi\epsilon}{(\epsilon^2 + 4\pi^2(x^2+y^2))^{3/2}}. \tag{51}$$

It is well known that $\delta_\epsilon(x,y)$ tends to 0 as $\epsilon \rightarrow 0$ at any point $(x,y) \neq (0,0)$.

IV. DISCUSSIONS AND CONCLUSION

There are relative merits and drawbacks associated with different limit methods for handling the case that $\hat{f}(u, \nu)$ is not absolutely integrable. Given comparable parameters, the method of limited bandwidth tends to produce finer spatial resolution, higher image noise, and stronger edge ringing, while the Abel method of summability may result in smoother profiles at the cost of poorer spatial resolution. A heuristic way to define the comparability of the parameters with the two methods may be to request that the area after hard/soft spectral truncation be identical.

Mathematically, it is requested that

$$\int_{-W}^W |w| dw = \int_{-\infty}^{\infty} |w| e^{-\epsilon|w|} dw, \tag{52}$$

which is equivalent to

$$\epsilon = \frac{\sqrt{2}}{W} \text{ or } W = \frac{\sqrt{2}}{\epsilon}. \tag{53}$$

Because $f_W(x,y)$ is a partial sum of a Fourier series, it exhibits the Gibbs phenomenon around discontinuous points. An example is a reconstructed unit disk function for $W = 10$, as shown in Fig. 1. On the other hand, the Gibbs phenomenon does not occur with the Abel method of summability, as demonstrated by $f_\epsilon(x,y)$ with $\epsilon = 0.1\sqrt{2} \approx 0.1414$ in Fig. 2. However, the sharpness of the slope on the unit circle is better in Fig. 1 than that in Fig. 2, which indicates better spatial resolution in the former than that in the latter. Quantitatively, the magnitude of the gradient of $f_W(x,y)$ on the unit circle is computed as follows:

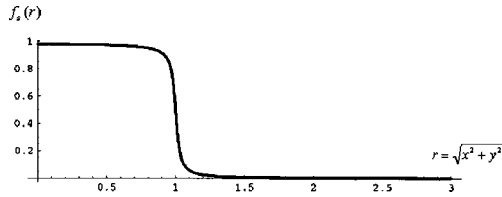


FIG. 1. Radial profile of a unit disk reconstructed using the method of limited bandwidth.

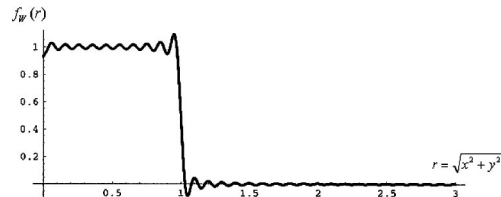


FIG. 2. Radial profile of a unit disk reconstructed using the Abel method of summability.

$$\begin{aligned}
 |\text{grad}[f_w(r)]| &= \left| \int_0^{2\pi W} J_1(w)J_0'(w)w \, dw \right| \\
 &= \int_0^{2\pi W} J_1^2(w)w \, dw \\
 &= 2\pi^2 W^2 [J_1^2(2\pi W) - J_0(2\pi W)J_2(2\pi W)],
 \end{aligned}
 \tag{54}$$

and its counterpart is

$$\begin{aligned}
 |\text{grad}[f_ε(r)]| &= \left| \int_0^\infty e^{-εw/2\pi} J_1(w)J_0'(w)w \, dw \right| \\
 &= \int_0^\infty e^{-εw/2\pi} J_1^2(w)w \, dw \\
 &= \frac{24\pi^4}{\epsilon^4} {}_2F_1\left(\frac{3}{2}, \frac{5}{2}; 3; -\frac{16\pi^2}{\epsilon^2}\right) \\
 &= 6\pi^4 W^4 {}_2F_1\left(\frac{3}{2}, \frac{5}{2}; 3; -8\pi^2 W^2\right).
 \end{aligned}
 \tag{55}$$

It can be shown that for $W > \frac{1}{3}$, we have

$$|\text{grad}[f_w(r)]| > |\text{grad}[f_ε(r)]|.
 \tag{56}$$

The current choice by CT manufacturers is based on the method of limited bandwidth and allows various degrees of modifications on the associated ramp filter, while the Abel method of summability remains an interesting theoretical possibility. The popularity of the method of limited bandwidth is due to the discrete detection technology and the Shannon sampling theorem. However, it is well known that the Fourier spectrum spreads over the whole space for any spatial function finitely supported. Suppose that we can record projection data continuously or extrapolate the Fourier spectrum well beyond the Nyquist bandwidth imposed by the sampling rate, the Abel method of summability may

have some practical merits. In addition to the methods we have discussed, other methods are also possible, based on various other ways to do the intermediate integrals, which should be equivalent to using approximate delta function of different types.⁷

In conclusion, for the method of limited bandwidth we have proved a pointwise limit theorem for a general class of functions. Our results have improved the understanding on filtered backprojection in CT. Although our work has been done in the parallel beam geometry, the findings are instructive for the divergent beam geometry. Further work is underway to extend the theory and explore its practical applications.

ACKNOWLEDGMENTS

The work is partially supported by NIH Grant No. (RO1 DC03590) and a grant from the Carver Scientific Research Initiative Grant Program. The authors thank Seung Wook Lee, John Meinel, and Xiang Li with the CT/Micro-CT Lab, University of Iowa, for discussions, and are grateful to anonymous reviewers for constructive critiques.

^aElectronic mail: yangbo-ye@uiowa.edu
^bElectronic mail: jiehua-zhu@uiowa.edu
^cElectronic mail: ge-wang@uiowa.edu

¹A. C. Kak and M. Slaney, *Principles of Computerized Tomographic Imaging* (Society for Industrial and Applied Mathematics, Philadelphia, 2001).
²F. Natterer, *The Mathematics of Computerized Tomography* (Society for Industrial and Applied Mathematics, Philadelphia, 2001).
³E. M. Stein and G. Weiss, *Introduction to Fourier Analysis on Euclidean Spaces* (Princeton University Press, Princeton, 1971).
⁴M. J. Lighthill, *An Introduction to Fourier Analysis and Generalized Functions* (Cambridge University Press, Great Britain, 1958).
⁵H. Bateman, *Tables of Integral Transforms* (McGraw-Hill, New York, 1954), Vol. I.
⁶H. Bateman, *Higher Transcendental Functions* (McGraw-Hill, New York, 1953), Vol. II.
⁷G. W. Wei, "Discrete singular convolution for the solution of Fokker-Planck equation," *J. Chem. Phys.* **110**, 8930–8942 (1999).
⁸F. Natterer, "Numerical methods in tomography," 1998, <http://www.math.uni-muenster.de/math/inst/num/Preprints/>.